Bioelectrochemistry 111 (2016) 49–56

Contents lists available at ScienceDirect

Bioelectrochemistry

journal homepage: www.elsevier.com/locate/bioelechem

Internal configuration and electric potential in planar negatively charged lipid head group region in contact with ionic solution

Alenka Maček Lebar [a,1], Aljaž Velikonja [a,1], Peter Kramar [a], Aleš Iglič [b,*]

[a] Laboratory of Biocybernetics, Faculty of Electrical Engineering, University of Ljubljana, Tržaška 25, SI-1000 Ljubljana, Slovenia
[b] Laboratory of Biophysics, Faculty of Electrical Engineering, University of Ljubljana, Tržaška 25, SI-1000 Ljubljana, Slovenia

ARTICLE INFO

Article history:
Received 12 August 2015
Received in revised form 19 April 2016
Accepted 19 April 2016
Available online 30 April 2016

Keywords:
MLPB model
Electric double layer
Ionic solution
MD simulations
1-palmitoyl-3-oleoyl-*sn*-glycero-3-phosphatidylserine bilayer
Water dipole ordering

ABSTRACT

The lipid bilayer composed of negatively charged lipid 1-palmitoyl-3-oleoyl-*sn*-glycero-3-phosphatidylserine (POPS) in contact with an aqueous solution of monovalent salt ions was studied theoretically by using the mean-field modified Langevin–Poisson–Boltzmann (MLPB) model. The MLPB results were tested by using molecular dynamic (MD) simulations. In the MLPB model the charge distribution of POPS head groups is theoretically described by the negatively charged surface which accounts for negatively charged phosphate groups, while the positively charged amino groups and negatively charged carboxylate groups are assumed to be fixed on the rod-like structures with rotational degree of freedom.

The spatial variation of relative permittivity, which is not considered in the well-known Gouy–Chapman (GC) model or in MD simulations, is thoroughly derived within a strict statistical mechanical approach. Therefore, the spatial dependence and magnitude of electric potential within the lipid head group region and its close vicinity are considerably different in the MLPB model from the GC model.

The influence of the bulk salt concentration and temperature on the number density profiles of counter-ions and co-ions in the lipid head group region and aqueous solution along with the probability density function for the lipid head group orientation angle was compared and found to be in qualitative agreement in the MLPB and MD models.

1. Introduction

Accumulation of opposite charged ions (counter-ions) and depletion of the ions with the charge of the same sign (co-ions) in the vicinity of a charged surface in contact with electrolyte solution results in the creation of an electric double layer (EDL) [1,2,3,4,5,6,7,8,9]. In biological system EDL plays an important role in cell membrane functions, like transmembrane transport and protein binding [10,11,12,13]. In the past, many different EDL theories have been proposed to describe the electrostatics of the cell membrane or artificial lipid membranes in contact with electrolyte solution [3,8,11]. Hermann von Helmholtz was the first who started to investigate EDL properties in the middle of 19th century [14,15]. Although Helmholtz's model qualitatively predicts some important properties of EDL, such as for example the order of magnitude of the potential near the charged surface, it is based on a few incorrect assumptions. Among others in the Helmholtz model the ion number density is considered to be constant and the thermal motion of the ions is not taken into account [10]. In the beginning of the 20th century Louis Gouy and Leonard Chapman, independently of each other, upgraded the Helmholtz's model of EDL within so-called Gouy–Chapman's (GC) model by considering the Boltzmann space distribution of the counter-ions and co-ions in Poisson equation [1,16,17,18]. A decade later Peter Joseph William Debye and Erich Hückel generalized GC model [1,18,19].

Stern [20] was the first who incorporated the finite size of ions in the EDL model by assuming the distance of the closest approach of counter-ions to the charged surface [13,21]. A more sophisticated approach to take into account the finite size of ions in the EDL (Wicke–Eigen model) was first discussed by Bikerman in [2] and then actually derived by Wicke and Eigen [22]. Since then many other generalized EDL models appeared which took into account the finite-size of ions by using different theoretical approaches [4,5,7,23,24,25,26,27,28,29,30,31,32,33].

Most of the mean-field theoretical models of EDL assume space independent relative permittivity throughout the whole electrolyte solution, accordingly the relative permittivity is considered as a constant in the Poisson–Boltzmann (PB) equation (for review see [1,3,7,8,11]). A constant relative permittivity is a relatively good approximation for small magnitudes of surface charge density, but not for higher magnitudes of surface charge density where a substantial decrease of relative permittivity in the vicinity of the charged surface in contact with electrolyte solution was predicted [8,9,13,34,35,36,37,38,39].

* Corresponding author.
E-mail address: ales.iglic@fe.uni-lj.si (A. Iglič).
[1] First and the second author equally shares the first authorship.

http://dx.doi.org/10.1016/j.bioelechem.2016.04.006
1567-5394/

Recently, a simple mean-field generalised Langevin–Bikerman model of the EDL was developed by Gongadze and Iglič [40] (GI model) which encapsulate both the excluded volume effect (finite size of ions) and the orientational ordering of water dipoles, considered as point-like dipoles at the centres of the spheres with permittivity equal to the square of the optical refractive index of water. Within the GI model, the mutual influence of the water molecules was taken into account by means of the cavity field [40]. The GI model predicts the space dependence of relative permittivity [8,40] and can be considered as a generalization of the previous Langevin–Poisson–Boltzmann's (LPB) model for point-like ions [38].

Electrostatic fields that are associated with the cell membrane arise mainly from charged phospholipid head groups and proteins. In the hydrophobic core of the membrane the net charge density is essentially zero. The net charge on the membrane is dependent on the pH and ionic composition of the adjacent solution phase. In physiological conditions, virtually all cells possess a negative membrane potential resulting from the predominance of negatively charged lipids. The negative charge on the membranes of mammalian cells is mainly a contribution of phosphatidylserines (PS), that typically constitute 2–10% of total phospholipids in most membranes [41]. Due to their important role in various cellular functions and in raft formation glycolipids, in particular gangliosides as for example GM1 [42], that contain one or more negatively charged sialic acid groups, also cannot be neglected [42,43,44], although they are present in much smaller proportion, only about 2% of the lipid in most plasma membranes. Lipid, glycolipids, protein, and ion contributions together result in electric potentials of −8 mV to −30 mV as found from electrophoretic mobility [45] and other types of measurements [46].

Additionally to the regulation of cell membrane surface charge, PS have been found to act as an important cofactor for virus infection, promoting vesicle endocytosis and fusion events, and are required for optimal protein targeting and activation during cell division and initiate the pathway of programmed cell death [47,48,49,50]. The understanding of the interactions of PS with cations and anions in ionic solution, therefore, contributes to better understanding of many membrane-mediated processes. Mostly, these interactions are studied by molecular dynamics (MD) computer simulation, which is an efficacious, but computational power demanding technique. The importance, prevalence and precision of MD simulations are growing, but the ion/lipid interactions for anionic lipids are still not fully understand. The reason might be in the ambiguous parameters and rules that are used for describing and calculating electrostatic interactions [51,52]. Therefore, theoretical models, like the MLPB model, can be useful in elucidating certain basic physical mechanisms that govern the interactions between anionic lipids and ions. Although the MLPB model presents a considerable simplification of the 3-D configuration of the lipid bilayer head group region in contact with ionic solution, it explicitly takes into account the spatial dependence of permittivity in the lipid bilayer head group region and its vicinity, derived within a self-consistent statistical mechanical approach, which is not the case in MD model.

In the present work we focused on the 1-palmitoyl-3-oleoyl-*sn*-glycero-3-phosphatidylserine (POPS) lipid (bi)layer in contact with electrolyte solution containing monovalent co-ions and monovalent counter-ions (e.g. NaCl). The POPS lipid molecule possesses a negatively charged PS head group. We included the charged structure of the PS lipid head groups in the modified LPB (MLPB) model [8,53] and compared the ion/lipid interactions obtained by this model with the results of MD simulations.

2. Methods

2.1. Theoretical model

The POPS lipid bilayer in contact with an ionic solution is theoretically described by using the modified Langevin–Poisson–Boltzmann (MLPB) model [38,53]. The MLPB model takes into account the cavity field in the saturation regimen, electronic polarization of water dipoles [38,40,54,55] and finite volumes of the amino (N) and carboxylate (O) parts of the lipid head groups. The finite volumes of other particles are not taken into account. Schematic presentation of the model is given in Schematic 1. The negatively charged phosphate (P) groups of the POPS molecules are described by the negative surface charge density $\sigma = -\frac{e_0}{a_0}$ at $x = 0$, where a_0 is area per lipid molecule and e_0 is an elementary charge. Within our model the Poisson equation can be written as [56]:

$$\frac{d}{dx}\left[\varepsilon_0\varepsilon_r(x)\frac{d\phi(x)}{dx}\right] = 2e_0n_0\sinh(e_0\phi(x)\beta) - \frac{e_0\mathcal{P}_1(x)}{D_1a_0} + \frac{e_0\mathcal{P}_2(x)}{D_2a_0}. \quad (1)$$

On the left side of Eq. (1), $\phi(x)$ denotes the electric potential, ε_0 is permittivity of free space and $\varepsilon_r(x)$ is spatial depended relative permittivity of ionic solution. The first summand on the right side of the equation describes the macroscopic volume charge density of co-ions and counter-ions in ionic solution, which are assumed to be distributed according to Boltzmann distribution function; n_0 is bulk number density of salt co-ions and counter-ions and $\beta = 1/kT$, and kT is the thermal energy. By the second two terms we described the macroscopic volume charge density of positively charged N groups and negatively charged O groups; $\mathcal{P}_1(x)$ is probability density function indicating the probability that the positive charge is located at the distance x from the negatively charged surface at $x = 0$ in the region $0 < x \le D_1$ and $\mathcal{P}_2(x)$ is probability density function indicating the probability that the negative charge is located at the distance x from the negatively charged surface at $x = 0$ in the region $0 < x \le D_2$:

$$\mathcal{P}_i(x) = \Lambda_i \frac{\alpha\exp\left(e_0\left(1-\frac{D_1}{D_2}\right)\beta x\mathrm{d}\phi/\mathrm{d}x\right)}{\alpha\exp\left(e_0\left(1-\frac{D_1}{D_2}\right)\beta x\mathrm{d}\phi/\mathrm{d}x\right)+1}, i = 1,2, \quad (2)$$

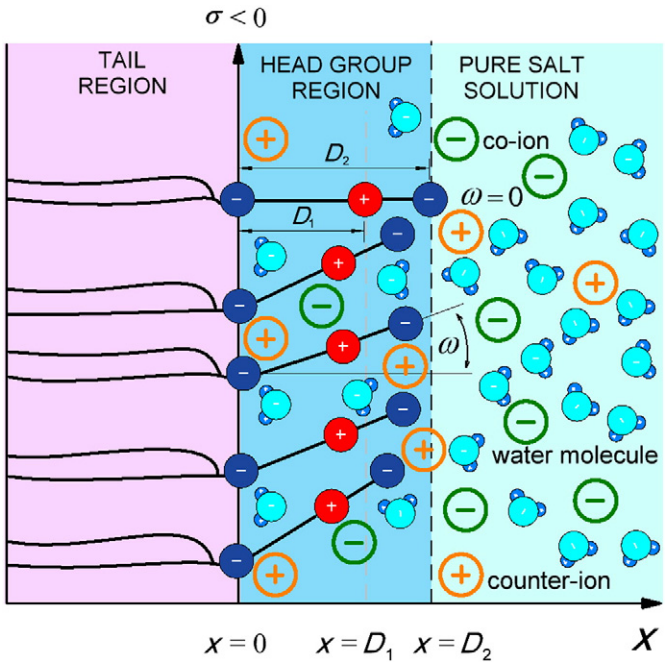

Schematic 1. Schematic presentation of the MLPB model of POPS layer in contact with ionic solution containing monovalent co-ions and monovalent counter-ions. Phosphate groups at $x = 0$ represent negatively charged surface described by the negative surface charge density σ. Other two groups of the lipid head groups, i.e. amino (positive) group and carboxylate (negative) group, penetrate into ionic solution. D_1 and D_2 are the distances to the amino and carboxylate groups from the negatively charged surface at $x = 0$, respectively. ω is the lipid head group orientation angle measured relative to the normal to the plane $x = 0$.

where we assumed $e_0\phi(x) - e_0\phi(x-\Delta x) \simeq e_0\Delta x \mathrm{d}\phi/\mathrm{d}x$ and $\Delta x = (1-\frac{D_1}{D_2})x$. Distances D_1 and D_2 are presented in Schematic 1; where D_1 is the distance between P and N group and D_2 is the distance between P and O group. Parameter α denotes the volume ratio between the charged lipid head groups (N and O groups) and the ionic solution inside the head group region. The values of Λ_i are calculated iteratively by numerical procedure until the normalization condition are met:

$$\frac{1}{D_i}\int_0^{D_i} \mathcal{P}_i(x)dx = 1, i = 1,2. \tag{3}$$

The boundary conditions are:

$$\frac{\mathrm{d}\phi}{\mathrm{d}x}(x=0) = -\frac{\sigma}{\varepsilon_0\varepsilon_r(x=0)}, \tag{4}$$

$$\frac{\mathrm{d}\phi}{\mathrm{d}x}(x\to\infty) = 0, \tag{5}$$

$$\phi\,(x = D_{1-}) = \phi\,(x = D_{1+}), \tag{6}$$

$$\varepsilon_r\,(x = D_{1-})\frac{\mathrm{d}\phi}{\mathrm{d}x}\,(x = D_{1-}) = \varepsilon_r\,(x = D_{1+})\frac{\mathrm{d}\phi}{\mathrm{d}x}\,(x = D_{1+}), \tag{7}$$

$$\phi(x = D_{2-}) = \phi(x = D_{2+}), \tag{8}$$

$$\varepsilon_r\,(x = D_{2-})\frac{\mathrm{d}\phi}{\mathrm{d}x}\,(x = D_{2-}) = \varepsilon_r\,(x = D_{2+})\frac{\mathrm{d}\phi}{\mathrm{d}x}\,(x = D_{2+}), \tag{9}$$

where in Eq. (4) the negative surface charge density of phosphate lipid group at $x=0$ is σ. Eq. (5) defines the electric field $E(x\to\infty)=0$ far away from the negatively charged surface at $x=0$. Eqs. (6) and (8) describe continuity of potential $\phi(x)$ at $x=D_1$ and $x=D_2$, respectively, while Eqs. (7) and (9) describe continuity of electric field $E(x)$ at the same borders (see also Schematic 1).

Eq. (1) was solved using standard implemented function for multi-boundary value problems (bvp4c) in Matlab2012b where the value $\varepsilon_r(x)$ was calculated in iteration process outside of bvp4c function. The $\varepsilon_r(x)$ within MLPB model is [38,53]:

$$\varepsilon_r(x) = n^2 + \frac{n_{0w}p_0}{\varepsilon_0}\left(\frac{2+n^2}{3}\right)\frac{\mathcal{L}(\gamma p_0 E(x)\beta)}{E(x)}, \tag{10}$$

where n is refractive index of water, n_{0w} is bulk concentration of water, p_0 is the dipole moment of water, $\mathcal{L}(u) = (coth(u) - 1/u)$ is the Langevin function, $\gamma = (3/2)((2+n^2)/3)$ and $E(x) = |\phi(x)'|$ is the magnitude of the electric field.

Number density profiles $n_+(x)$ (counter-ions) and $n_-(x)$ (co-ions) are calculated according to Boltzmann distribution function [3,4,5,7,11,57]:

$$n_+(x) = n_0\exp(-e_0\phi(x)\beta), \tag{11}$$

$$n_-(x) = n_0\exp(e_0\phi(x)\beta). \tag{12}$$

The average lipid head group orientation angle $\langle\omega\rangle$ (see also Schematic 1) is calculated as:

$$\omega = \frac{\int_0^{\pi/2} \omega\mathcal{P}_i(D_i\cos\omega)D_i\sin\omega\mathrm{d}\omega}{\int_0^{\pi/2} \mathcal{P}_i(D_i\cos\omega)D_i\sin\omega\mathrm{d}\omega}, i = 1,2, \tag{13}$$

where the probability density functions $\mathcal{P}_i(x)$ as a function of $x = D_i\cos\omega$ are defined above by Eq. (2). From Eq. (13) follows the equation for probability density functions for lipid head group orientation angle in the form:

$$\mathcal{F}_i(\omega) = \frac{\mathcal{P}_i(D_i\cos\omega)\sin\omega}{\int_0^{\pi/2} \mathcal{P}_i(D_i\cos\omega)\sin\omega\mathrm{d}\omega}, i = 1,2. \tag{14}$$

$\mathcal{F}_1(\omega)$ is the probability density function of the amino (N) group orientation angle and $\mathcal{F}_2(\omega)$ is the probability density function of the carboxylate (O) group orientation angle. The final distribution of the lipid head group orientation angle $\mathcal{F}(\omega)$ as a result of the MLPB model was calculated as an average of $\mathcal{F}_1(\omega)$ and $\mathcal{F}_2(\omega)$.

2.2. MD simulations

The molecular dynamics (MD) model of the planar lipid bilayer was constructed in the NAMD program using an all molecule performance CHARMM 27 force field. The model consists of 392 lipid units of POPS and 39,200 water molecules. The solvent was 250 mM NaCl modeled by 576 Sodium and 184 Chloride ions [58,59]. The chemical bonds between the hydrogen and heavy atoms were constrained to their equilibrium values. Long-range electrostatic forces were taken into account using a fast implementation of the particle mesh Ewald (PME) method [60,61] with a cutoff distance of 1.1 nm. The model was examined at constant pressure (1.013×10^5 Pa) and constant temperature (300 K) employing Langevin dynamics and the Langevin piston method. The equations of motion were integrated using the multiple time-step algorithm. A time step of 2.0 fs was employed. Short- and long-range forces were calculated every one and two time steps, respectively.

The model was equilibrated and followed at 30 ns intervals. The last 15 ns of the simulation was used for extraction of the position of the P atom in the phosphate group, the N atom in amino group and the O atom in carboxylate group in all 392 lipids. The positions of the atoms in 1500 simulation frames were exported to Matlab2012b.

2.3. Interrelation between MD simulations and the MLPB model

We calculated the distribution of vectors connecting P and N atoms (PN) and the distribution of vectors connecting P and O atoms (PO) obtained by MD simulation. An average PN vector was 0.43 nm long and formed an angle of 71° with a normal of planar lipid bilayer plane, while an average PO vector was 0.59 nm long and formed an angle of 68° with a normal of planar lipid bilayer's plane. To determine a parameter D_1 in the MLPB model (Eq. (1)) we calculated the scalar projection of an average PN vector in a direction normal to the planar lipid bilayer's plane (see Schematic 2). Similarly, a parameter D_2 in MLPB model (Eq. (1)) was obtained by calculation of the scalar projection of an average PO vector in a direction normal to the planar lipid bilayer's plane. The distribution of lipid head group orientation angle $\mathcal{F}(\omega)$ as a result of MD simulations was obtained considering all PO vectors by calculation of their angles with respect to normal to the planar lipid bilayer's plane.

3. Results and discussion

The number density profile of counter-ions and co-ions as a function of the distance from the negatively charged surface at $x=0$ calculated within the MLPB model and then tested by MD simulation is given in Fig. 3. It can be seen that the results of both models show a high accumulation of counter-ions in the vicinity of the negatively charged surface at $x=0$. In MD simulation, the resulting number density profile of counter-ions (Na^+) is a smooth almost symmetrical curve with a maximum in the carboxylate group region ($x=D_2$). The results of our MD simulation are in line with the results of Pan et al. [62]. They found that counter-ions interact most strongly with the terminal carboxylic

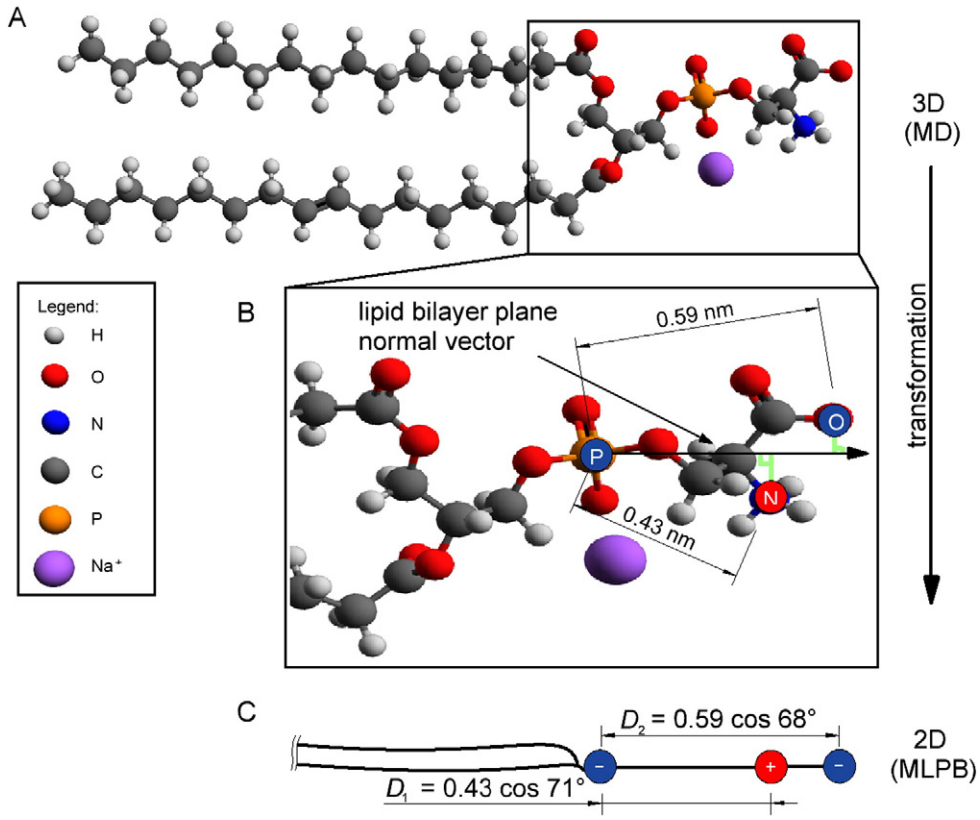

Schematic 2. Single POPS lipid molecule obtained in MD simulation and MLPB model: (A) schematic 3D presentation of POPS molecule in MD, (B) POPS molecule with the values of average distances between P, N and O atoms obtained in MD simulation and (C) model of POPS molecule used in the MLPB approach. D_1 represents the distance between phosphate group and amino group, while D_2 represents the distance between the phosphate group and carboxylate group, calculated as projection of the vector between P and N atoms and vector between P and O atoms in a direction normal to the lipid bilayer plane, respectively.

oxygen, followed by the phosphate oxygen and lastly, by the backbone oxygen in the ester region. Namely, in MD simulation counter-ions are able to penetrate into the ester region of the planar lipid bilayer, so the number of counter-ions continuously drop to zero at the inner side of the phosphate plane. In the MLPB model the phosphate atoms are presented as a negatively charged surface. It is obvious that counter-ions $(n+)$ accumulate in phosphate plane outer vicinity and that their number is larger than in the MD simulation case, because they cannot penetrate on the opposite side of the phosphate plane. The density of counter-ions obtained by MD simulation (Na^+) and the MLPB model $(n+)$ shows the best agreement at the maximum of the number density profile of the counter-ions obtained by MD simulations, in the vicinity of the terminal carboxylic oxygen ($x = D_2$). Further in solution ($x > D_2$) the MD model predicts a higher number of counter-ions than the MLPB model. The reason for this discrepancy lies mainly in two facts. First, the boundary between the lipid head groups and the ionic solution obtained in MD simulation is rather diffuse and, therefore, even phosphate atoms do not lie in the plane as is predicted in the MLPB model. Secondly, the usage of average PN and PO vectors in the MLPB model allows location of positive charges (N) just in the interval $0 < x \le D_1$ and location of negative charges (O) just in the interval $0 < x \le D_2$. So, any location of N and O parts of the lipid head groups deeper in ionic solutions is not predicted, and therefore also the calculated distribution of counter-ions is squeezed.

The number density of co-ions of the MLPB model decreases almost to zero in the vicinity of the terminal carboxylic oxygen ($x = D_2$), while in MD simulation small amounts of co-ions are present in the terminal carboxylic oxygen region (Fig. 3). Due to the small number density of co-ions in the head group region, just a few co-ions can increase the number density in the case of MD simulation. The differences in the distributions are also the result of the difference in the basics of both models; again in the MLPB model the co-ions cannot penetrate on the opposite side of the negatively charged plane (phosphate plane). In MD simulation some co-ions can also be present also in the ester region of the planar lipid bilayer ($x < 0$), therefore, in MD simulation the number density of chloride ions even at $x = 0$ is not equal to zero. Far away from the lipid head groups $x >> D_2$ (i.e. far away from the carboxylic oxygen region) the number densities of co-ions $(n-)$ and counter-ions $(n+)$ in MLPB and MD approach their bulk values, fulfilling the electroneutrality condition.

The influence of the bulk salt concentration on the number density profiles of counter-ions $(n+)$ and co-ions $(n-)$ calculated within the MLPB model is shown in Fig. 4. The molar concentrations of salt (e.g. NaCl) employed were 25 mM, 150 mM and 250 mM. As expected the main behaviour of the number density profiles of both ions is not changed, only the bulk values are different. The number density profiles of counter-ions $(n+)$ and co-ions $(n-)$ were also calculated for various temperatures. The temperature in the MLPB model was varied between 290 K and 315 K in increments of 5 K. The results showed that temperature has no effect on the number density profiles of counter-ions $(n+)$ and co-ions $(n-)$ in the studied temperature range (data not shown).

The probability density function $\mathcal{F}(\omega)$ for lipid head group orientation angle ω calculated within the MLPB model and obtained from MD simulation can be seen in Fig. 5. The probability density function $\mathcal{F}(\omega)$ calculated within the MLPB model is smooth, increases with growing orientation angle ω, reaches its maximum between 77° and 79.5° and then starts to decrease. On average more lipid head groups are strongly tilted towards the lipid bilayer surface than nearly fully extended in a perpendicular direction to the lipid bilayer's plane. There is relatively good agreement between predictions of the MLPB model and MD simulation. The discrepancy is the largest at smaller angles, where the MLPB model predicts more slightly tilted molecules than the MD

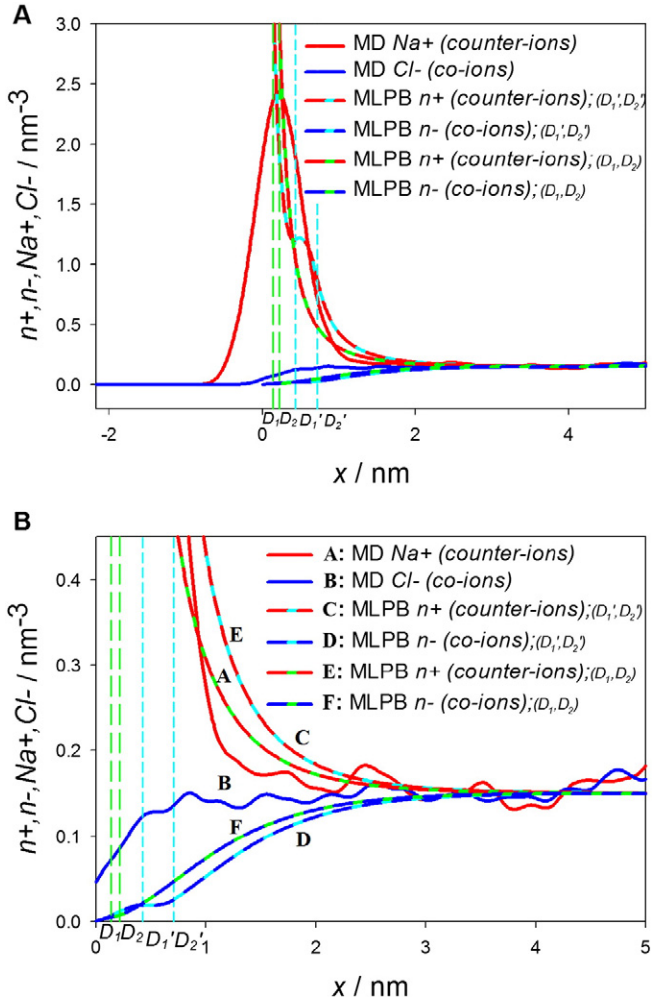

Fig. 3. (A) The number density profile of counter-ions and co-ions as a function of the distance from the negatively charged surface at $x=0$ calculated by MLPB model (dashed plots) at two different distances (D_1,D_2); green lines and (D_1',D_2'); cyan lines, between phosphate and amino groups from the negatively charged surface at $x=0$, and obtained from MD simulations (solid lines). The values of parameters in the MLPB are: $T=300$ K, $\sigma=-e_0/a_0$, $a_0=0.53$ nm^2, dipole moment of water $p_0=3.1$ Debye, $D_1=0.14$ nm, $D_2=0.22$ nm, $D_1'=0.43$ nm, $D_2'=0.71$ nm, $\alpha=1$, the bulk concentration of salt $n_0/N_A=0.25$ mol/l, the bulk concentration of water $n_{0w}/N_A=55$ mol/l, where N_A is Avogadro number. (B) Emphasized part of the number density profile in the vicinity of the negatively charged surface at $x=0$.

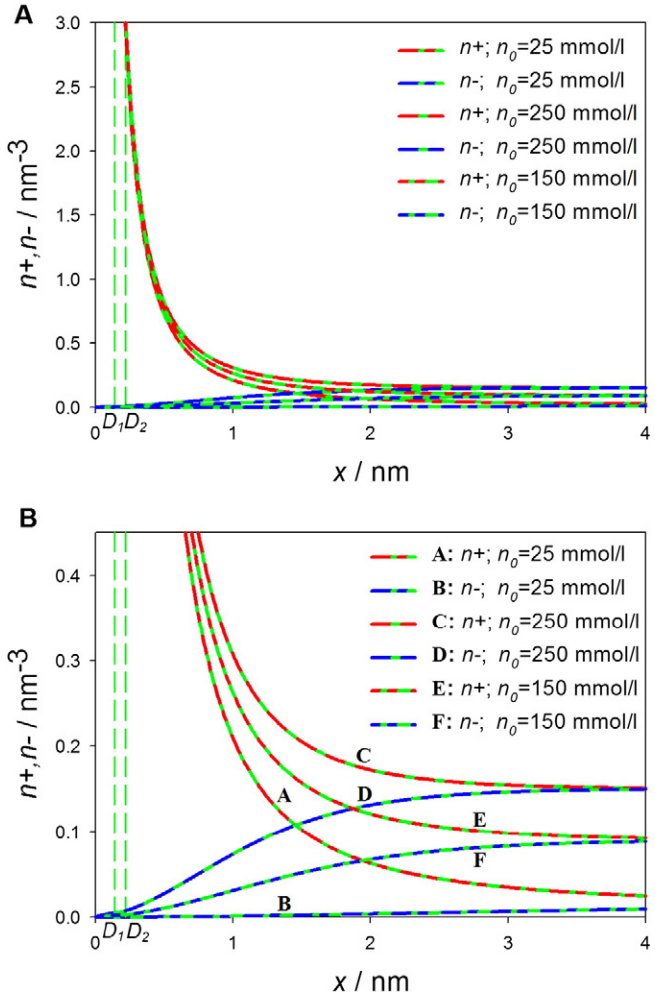

Fig. 4. (A) The number density profile of counter-ions ($n+$) and co-ions ($n-$) as a function of the distance from the negatively charged surface at $x=0$ calculated by MLPB model at the distances D_1 and D_2 (long dashed green vertical lines), corresponding to the distances between the amino (N) and carboxylate (O) group from the negatively charged surface ($x=0$) at different bulk concentrations of salt. The values of other parameters MLPB are: $T=300$ K, $\sigma=-e_0/a_0$, $a_0=0.53$ nm^2, dipole moment of water $p_0=3.1$ Debye, $D_1=0.14$ nm, $D_2=0.22$ nm, $\alpha=1$, the bulk concentration of water $n_{0w}/N_A=55$ mol/l, where N_A is Avogadro number. (B) Emphasized part of the number density profile in the vicinity of the negatively charged surface at $x=0$.

simulation. It should be noted that lipid head group orientation angles obtained in MD simulation are also larger than 90°, while all the molecules in the MLPB model should arrange their heads in an angel between 0° and 90°.

The usage of average PN and PO vectors in the MLPB model restricts the locations of positive charges (N) in the interval $0<x\leq D_1$ and locations of negative charges (O) on the interval $0<x\leq D_2$ (see Fig. 3). Therefore, any locations of the N and O parts of the lipid head groups deeper in the ionic solution are not predicted. In order to achieve all the possible positions of the charges in the MLPB model, the model was also run with limit (maximal) dimensions of PN and PO vectors, $D_1'=0.43$ nm and $D_2'=0.71$ nm, respectively.

The number density profile of counter-ions ($n+$) and co-ions ($n-$) as a function of the distance from the negatively charged surface at $x=0$ calculated within MLPB model, where limit dimensions were used, is given in Fig. 3. Indeed, using D_1' and D_2' in the MLPB model, better agreement in the number density of counter-ions ($n+$) in the ionic solution close to the lipid head group region (nearby D_2') is obtained. Moreover, the MLPB model predicts a little bit higher number of counter-ions ($n+$) even further into solution. Also, in this limit case the density of counter-ions obtained in MD simulation ($Na+$) and the MLPB model ($n+$) agrees in the vicinity of the average terminal carboxylic oxygen location ($x=D_2$), while in the region between average O locations (D_2) and limit N location (D_1') the MLPB model predicts a lower number of counter-ions ($n+$). As in the previous case, in the MLPB model counter-ions ($n+$) accumulate in the phosphate plane outer vicinity. In fact, the number density profile of counter-ions ($n+$) calculated within the MLPB model using limit parameters D_1' and D_2' seems to be bimodal, if penetration of couter-ions ($n+$) on the opposite side of the negatively charged plane were to be possible. The outer extreme is located 0.48 nm from the phosphate plane, or 2.68 nm from the lipid bilayer cleavage plane. Bimodal number density profile of counter-ions (Na^+) was obtained also in the MD simulations reported by Mukhopadhyay et al. [63] and Vanable et al. [52]. In both reports the phosphate peak is shifted towards the center of the bilayer; in MD simulation reported by Vanable et al. the inside peak is located between the ester and phosphate region, while in the report by Mukhopadhyay et al. the inside peak corresponds to the ester region and a minimum in bimodal distribution is shown between the phosphate and carboxylate regions. In both MD simulations the outer extreme is located approximately 2.7 nm from the lipid bilayer cleavage plane, but the extreme

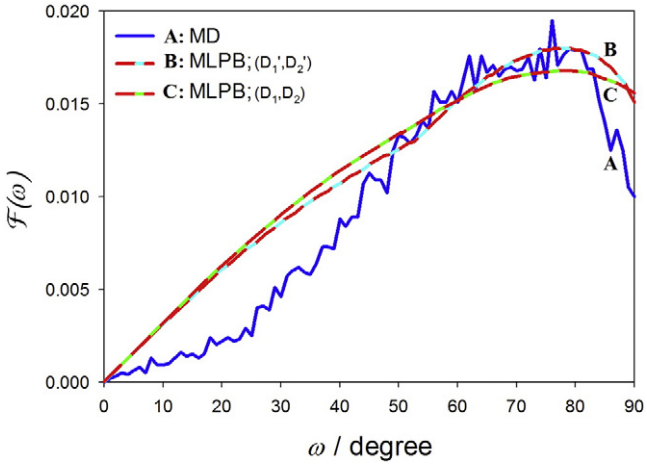

Fig. 5. The probability density function $\mathcal{F}(\omega)$ for the lipid head group orientation angle ω calculated within the MLPB (red dashed line) as an average of $\mathcal{F}_1(\omega)$ and $\mathcal{F}_2(\omega)$ (see Eq. (14)) at two distances (D_1, D_2); green lines — C plot and (D_1', D_2'); cyan lines — B plot, between phosphate and amino group from the negatively charged surface $(x=0)$, and obtained from MD simulations (blue solid line). The values of parameters in the MLPB model are the same as in Fig. 3. Note: The lipid head group orientation angle in MD is calculated between 0° and 180°, therefore the area under corresponding plot is less than 1.

value is considerably lower in the case reported by Vanable et al. The results obtained within the MLPB model are in good agreement with the report by Vanable et al., where they refined standardly used Lennard–Jones parameters in MD simulations and validated them with experimental measurements.

The number density of co-ions $(n-)$ within the MLPB model (see Fig. 3), where limit parameters D_1' and D_2' were used, decreases almost to zero already in the ionic solution close to the lipid head group region (near $x=D_2'$). Also, in this case just a few co-ions $(n-)$ are present in the head group region. The predicted head group region is larger and, therefore, also the discrepancy with the MD simulation results.

The influence of the bulk salt concentration on the number density profiles of counter-ions $(n+)$ and co-ions $(n-)$ calculated within the MLPB model, where limit parameters D_1' and D_2' were used, is shown in Fig. 6. The number density profiles of counter-ions $(n+)$ and co-ions $(n-)$ were calculated for 25 mM, 150 mM and 250 mM concentrations of salt (e.g. NaCl). Also, in this case the main behaviour of the number density profiles of both ions is not changed, only the bulk values are different. Again, the MLPB model run at various temperatures showed that temperature has no effect on the number density profiles of counter-ions $(n+)$ and co-ions $(n-)$ in the studied temperature range (290 K–315 K) (data not shown).

The probability density function $\mathcal{F}(\omega)$ for lipid head group orientation angle ω can be seen in Fig. 5. The probability density function $\mathcal{F}(\omega)$ calculated within the MLPB model increases with growing orientation angle ω, reaches its maximum between 76° and 79.5° and then starts to decrease. On average the agreement between the predictions of the MLPB model and MD simulation is better than in the case of average parameters D_1 and D_2, but the discrepancy is still present at smaller angles, where the MLPB model predicts more slightly inclined molecules than MD simulation.

4. Conclusion

In this study we developed a simple mean field MLPB model to study the electrostatic properties within the head group region of charged anionic lipid bilayer and its vicinity. The results of presented MLPB model were tested by corresponding MD simulation. Among others we calculated the counter-ions and co-ions number density profiles within and outside of the head group region and the probability density function

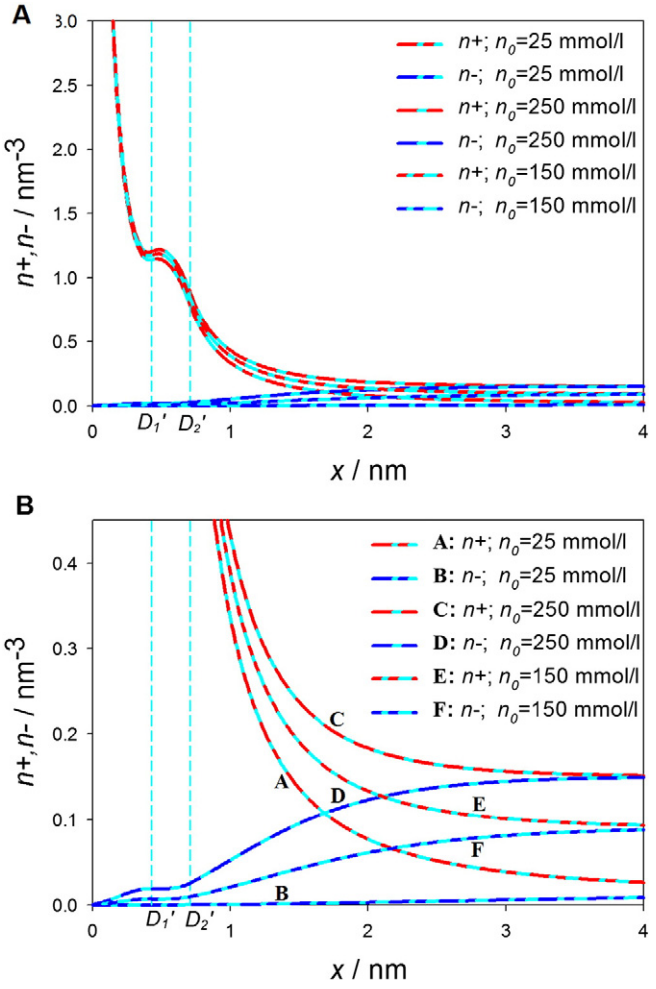

Fig. 6. (A) The number density profile of counter-ions $(n+)$ and co-ions $(n-)$ as a function of the distance from the negatively charged surface at $x=0$ calculated by MLPB model at the distances D_1' and D_2' (short dashed cyan vertical lines), corresponding to the distances between phosphate and amino group from the negatively charged surface $(x=0)$ at different bulk concentrations of salt. The values of other parameters in the MLPB are: $T=300$ K, $\sigma=-e_0/a_0$, $a_0=0.53$ nm^2, dipole moment of water $p_0=3.1$ Debye, $D_1'=0.43$ nm, $D_2'=0.71$ nm, $\alpha=1$, the bulk concentration of water $n_{0w}/N_A=55$ mol/l, where N_A is Avogadro number. (B) Emphasized part of the number density profile in the vicinity of the negatively charged surface at $x=0$.

for lipid head group orientation angle. In the presented mean-field MLPB model of the lipid bilayer in the contact with electrolyte solution, the charge distribution of the POPS head groups in lipid bilayer is theoretically described by the negatively charged planar surface which accounts for negatively charged phosphate groups, while the positively charged amino groups and negatively charged carboxylate groups of POPS head groups are assumed to be fixed on the rod-like structures with rotational degree of freedom. The MLPB model, based on a statistical-mechanical approach, takes into account the finite volumes of carboxylate and amino parts of the lipid head groups only, while the MD simulation takes into account the finite volumes of all the particles in the system. We have shown that the predictions of the MLPB model are in qualitative agreement with the MD simulations results.

The differences in the results obtained with MD simulations and the MLPB model can be attributed on the one hand to oversimplifications made in the MLPB model, especially in description of 3-D structure of lipid head group region and freedom of movement of atoms/molecules within this region. But on the other hand also to large numbers of poorly known parameters in MD model defined within Newton dynamics. Among other factors, the calculated distribution of counter-ions and co-ions in MD simulations depends highly on the type of applied force

fields, the model of electrostatic interactions, cutoff distance and the temperature of the simulation as well as combinations of these parameters [52,62,63]. In addition, in MD simulations the temperature, as thermodynamic/statistical mechanics parameter, is introduced via equipartition theorem, while at the same time the entropy is not taken into account, which is not a consistent approach. By neglecting the entropic contribution to the free energy in MD simulation, the energy of the system is minimized instead of the minimisation of the free energy (see for example Zelko et al. [64]).

Therefore, the mean-field nearly analytical models, like MLPB, may be of considerable importance in elucidating independently the effect of particular physical properties on the behaviour of complex systems such as the charged surface of lipid membranes. In this way certain basic insights in the physical mechanisms that govern the particular phenomena in biological system can be better understand and may also contribute to better understanding of the results of MD simulations.

As for example, in the MLBP model the spatial variation of relative permittivity in the system is derived within a strict statistical mechanical approach (see Eq. (10) and [8]), unlike MD models which assume that the constant relative permittivity or the spatial dependence of relative permittivity is approximated by phenomenological functions using poorly known parameters. This is an oversimplification which may strongly influence the calculated spatial dependence of the electric field, especially in the head group region of the lipid bilayer. Namely, it was shown theoretically and experimentally that the relative permittivity in the lipid head group region and its vicinity strongly varies (see [8,9,13,34,35,36,37,38,39] and the references therein). Unlike MD models, this phenomenon is well described within the MLPB model by using Eq. (10) derived within a thorough statistical mechanical approach. Note, that within the MD model the electric potential spatial dependence is calculated from a continuous Poisson equation by using the independently calculated volume charge density as the input data. In the MLPB model the Poisson equation and the volume charge distribution are calculated in self-consistent way.

The spatial variation of relative permittivity, which is also not considered in the traditionally used Gouy–Chapman (GC) model, makes the spatial dependence and magnitude of electric potential within the lipid head group region and its close vicinity considerably different in MLPB model to the GC model. Electric potential near the membranes and near the membrane-protein systems calculated in MD simulations are often verified by a GC model or Debye–Hückel's (DH) model which is similar to the GC model, but which also does not take into account the spatial variation of relative permittivity. Because the spatial variation of relative permittivity is not considered in GC and DH models, the calculated spatial dependence and magnitude of electric potential within the lipid head group region and its vicinity within the MLPB model considerably differs from the corresponding values determined by using the DH and GC model (see Fig. 7).

To conclude, our simple mean field MLPB model, which simultaneously takes into account the 3-D structure and the spatial dependent relative permittivity within the lipid head group region, both totally neglected within traditionally used GC and DH models, could be used to improve the analysis of experimental data in lipid electrochemistry. Accordingly, the application of the MLPB model instead of GC and DH models in the experimental evaluation of lipid bilayer surface potential and the electric potential within the bilayer head group region from the measured Zeta potentials or from the measured distribution of fluorescent and other types of markers between the lipid bilayer and bulk solution, may contribute substantially to more realistic values of experimentally determined lipid bilayer electric potentials.

Disclosure

The authors have no conflicts of interest to disclose in this work.

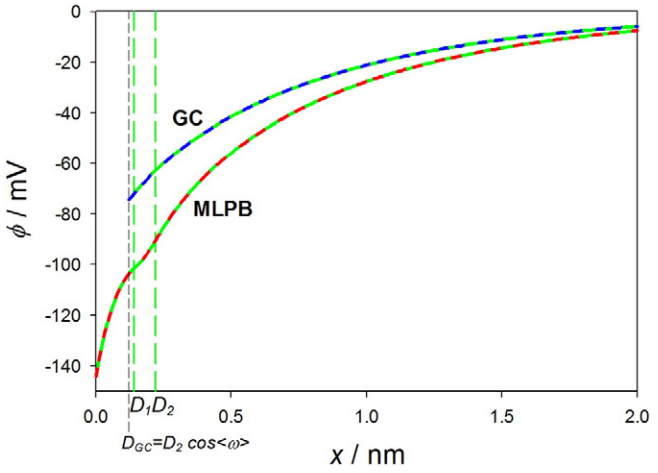

Fig. 7. Electrical potential ϕ as a function of the distance from the negatively charged surface at $x=0$ calculated within the MLPB model (A plot) and Gouy–Chapman (GC) model (B plot). Negatively charged plane for the GC model was set at the distance $D_{GC}=0.12$ nm, corresponding to the mean distance of carboxylate (O) parts of the lipid head groups from the negatively charged surface projected to the lipid bilayer's normal vector. The bulk concentration of salt is $n_0/N_A=0.15$ mol/l, while the values of other parameters are the same as in Fig. 4.

Acknowledgement

This work was partially supported by the Slovenian Research Agency (ARRS) (No. P2-0232, J5-7098, J1-6728 and P2-0249). Author AV was mainly supported by European social fund and SMARTEH d.o.o., Slovenia. Molecular Dynamics Simulations were performed using HPC resources from Arctur d.o.o., Slovenia. Authors thank Andraž Polak and Mounir Tarek for advises considering MD simulations. The research was conducted in the scope of the EBAM European Associated Laboratory (LEA).

References

[1] E.J.W. Verwey, J.T.G. Overbeek, J.T.G. Overbeek, Theory of the Stability of Lyophobic Colloids, Courier Dover Publications, 1999.
[2] J.J. Bikerman, Xxxix. Structure and capacity of electrical double layer, Philos. Mag. 33 (220) (1942) 384–397.
[3] G. Cevc, Membrane electrostatics, Biochim. Biophys. Acta 1031 (1990) 311–382.
[4] V. Kralj-Iglič, A. Iglič, A simple statistical mechanical approach to the free energy of the electric double layer including the excluded volume effect, J. Phys. II 6 (4) (1996) 477–491.
[5] S. Lamperski, C.W. Outhwaite, Exclusion volume term in the inhomogeneous Poisson–Boltzmann theory for high surface charge, Langmuir 18 (2002) 3423–3424.
[6] Z. Arsov, M. Rappolt, J. Grdodolnik, Weakened hydrogen bonds in water confined between lipid bilayers: the existence of a long-range attractive hydration force, Chem. Phys. Chem. 10 (9) (2009) 1438–1441.
[7] M. Bazant, M. Kilic, B. Storey, A. Ajdari, Advances in colloid and interface science, Adv. Colloid Interf. Sci. 152 (2009) 48.
[8] E. Gongadze, A. Velikonja, Š. Perutkova, P. Kramar, A. Maček-Lebar, V. Kralj-Iglič, A. Iglič, Ions and water molecules in an electrolyte solution in contact with charged and dipolar surfaces, Electrochim. Acta 126 (2014) 42–60.
[9] M.A. Quiroga, K.-H. Xue, T.-K. Nguyen, M. Tułodziecki, H. Huang, A.A. Franco, A multiscale model of electrochemical double layers in energy conversion and storage devices, J. Electrochem. Soc. 161 (8) (2014) E3302–E3310.
[10] M.E. Starzak, The Physical Chemistry of Membranes, Academic Press London, UK, 1984.
[11] S. McLaughlin, The electrostatic properties of membranes, Annu. Rev. Biophys. Biophys. Chem. 18 (1) (1989) 113–136.
[12] M. Kandušer, M. Fošnarič, M. Šentjurc, V. Kralj-Iglič, H. Hägerstrand, A. Iglič, D. Miklavčič, Effect of surfactant polyoxyethylene glycol (C12E8) on electroporation of cell line dc3f, Colloids Surf. A Physicochem. Eng. Asp. 214 (1) (2003) 205–217.
[13] H. Butt, K. Graf, M. Kappl, Physics and Chemistry of Interfaces, Weinheim, Wiley-VCH Verlag, 2003.
[14] H.v. Helmholtz, Über einige gesetze der vertheilung elektrischer ströme in körperlichen leitern mit anwendung auf die thierisch-elektrischen versuche, Ann. Phys. 165 (6) (1853) 211–233.
[15] H.v. Helmholtz, Studien über elektrische grenzschichten, Ann. Phys. Chem. 243 (1879) 337382.
[16] M.G. Gouy, Sur la constitution de la charge electrique la surface dun electrolyte, J. Phys. Radium (1910) 457–468.

[17] D.L. Chapman, A contribution to the theory of electrocapillarity, Philos. Mag. 6 (1913) 475–481.
[18] F. Fogolari, A. Brigo, H. Molinari, The Poisson–Boltzmann equation for biomolecular electrostatics: a tool for structural biology, J. Mol. Recognit. 15 (6) (2002) 377–392.
[19] P. Debye, E. Huckel, The theory of electrolytes. I. Lowering of freezing point and related phenomena, Phys. Z. 24 (9) (1923) 185–206.
[20] O. Stern, Zur theorie der elektrolytischen doppelschicht, Z. Elektrochem. Angew. Phys. Chem. 30 (21—22) (1924) 508–516.
[21] A. Velikonja, V. Kralj-Iglič, A. Iglič, On asymmetric shape of electric double layer capacitance curve, Int. J. Electrochem. Sci. 10 (2015) 1–7.
[22] E. Wicke, M. Eigen, Über den einflu des raumbedarfs von ionen in wässriger lösung auf ihre verteilung im elektrischen feld und ihre aktivit ätskoeffizienten, Z. Elektrochem. 56 (1952) 551–561.
[23] I. Borukhov, D. Andelman, H. Orland, Steric effects in electrolytes: a modified Poisson Boltzmann equation, Phys. Rev. Lett. 79 (1997) 435–438.
[24] S.W. Kenkel, J.R. Macdonald, A lattice model for the electrical double layer using finite-length dipoles, J. Chem. Phys. 81 (7) (1984) 3215–3221.
[25] P. Nielaba, F. Forstmann, Packing of ions near an electrolyte-electrode interface in the hnc/lmsa approximation to the rpm model, Chem. Phys. Lett. 117 (1) (1985) 46–48.
[26] C. Caccamo, G. Pizzimenti, L. Blum, An improved closure for the Born–Green–Yvon equation for the electric double layer, J. Chem. Phys. 84 (6) (1986) 3327–3335.
[27] R. Kjellander, S. Marčelja, Interaction of charged surfaces in electrolyte solutions, Chem. Phys. Lett. 127 (4) (1986) 402–407.
[28] M. Plischke, D. Henderson, Pair correlation functions and density profiles in the primitive model of the electric double layer, J. Chem. Phys. 88 (4) (1988) 2712–2718.
[29] L. Mier-y Teran, S. Suh, H.S. White, H. Davis, A nonlocal free-energy density-functional approximation for the electrical double layer, J. Chem. Phys. 92 (8) (1990) 5087–5098.
[30] V. Kralj-Iglič, B. Babnik, D.R. Gauger, S. May, A. Iglič, Quadrupolar ordering of phospholipid molecules in narrow necks of phospholipid vesicles, J. Stat. Phys. 125 (2006) 727–752, http://dx.doi.org/10.1007/s10955-006-9051-9.
[31] I. Bivas, Electrostatic and mechanical properties of a flat lipid bilayer containing ionic lipids, Colloids Surf. A 282-283 (2006) 423–434.
[32] I. Bivas, Y.A. Ermakov, Elasticity and electrostatics of amphiphilic layers, Adv. Planar Lipid Bilayers Liposomes 5 (2007) 313–343.
[33] E. Gongadze, A. Iglič, Asymmetric size of ions and orientational ordering of water dipoles in electric double layer model — an analytical mean-field approach, Electrochim. Acta 178 (2015) 541–545.
[34] C. Outhwaite, A treatment of solvent effects in the potential theory of electrolyte solutions, Mol. Phys. 31 (5) (1976) 1345–1357.
[35] C. Outhwaite, Towards a mean electrostatic potential treatment of an ion–dipole mixture or a dipolar system next to a plane wall, Mol. Phys. 48 (3) (1983) 599–614.
[36] T. Nagy, D. Henderson, D. Boda, Simulation of an electrical double layer model with a low dielectric layer between the electrode and the electrolyte, J. Phys. Chem. B 115 (39) (2011) 11409–11419.
[37] A. Iglič, E. Gongadze, K. Bohinc, Excluded volume effect and orientational ordering near charged surface in solution of ions and Langevin dipoles, Bioelectrochemistry 79 (2) (2010) 223–227.
[38] E. Gongadze, U. van Rienen, V. Kralj-Iglič, A. Iglič, Langevin Poisson–Boltzmann equation: point-like ions and water dipoles near charged membrane surface, Gen. Physiol. Biophys. 30 (2011) 130–137.
[39] R.P. Misra, S. Das, S.K. Mitra, Electric double layer force between charged surfaces: effect of solvent polarization, J. Chem. Phys. 138 (11) (2013) 114703.
[40] E. Gongadze, A. Iglič, Decrease of permittivity of an electrolyte solution near a charged surface due to saturation and excluded volume effects, Bioelectrochemistry 87 (2012) 199–203.
[41] J.E. Vance, Thematic review series: glycerolipids. Phosphatidylserine and phosphatidylethanolamine in mammalian cells: two metabolically related aminophospholipids, J. Lipid Res. 49 (8) (2008) 3047–3064.
[42] S.L. Frey, E.Y. Chi, C. Arratia, J. Majewski, K. Kjaer, K.Y.C. Lee, Condensing and fluidizing effects of ganglioside gm1 on phospholipid films, Biophys. J. 94 (8) (2008) 3047–3064.
[43] L. Mrwczynska, C. Lindqvist, A. Iglič, H. Hgerstrand, Spontaneous curvature of ganglioside gm1 — effect of cross-linking, Biochem. Biophys. Res. Commun. 422 (2012) 776–779.
[44] D. Kabaso, M. Lokar, V. Kralj-Iglič, P. Veranič, A. Iglič, Temperature and cholera toxin b are factors that influence formation of membrane nanotubes in RT4 and T24 urothelial cancer cell lines, Int. J. Nanomedicine 6 (2011) 495–509.
[45] A. Baszkin, W. Norde, Physical Chemistry of Biological Interfaces, CRC Press, 1999.
[46] A. Iglič, M. Brumen, S. Svetina, Determination of inner surface potential of erythrocyte membrane, Bioelectrochem. Bioenerg. 43 (1997) 97–103.
[47] M.K. Callahan, P.M. Popernack, S. Tsutsui, L. Truong, R.A. Schlegel, A.J. Henderson, Phosphatidylserine on hiv envelope is a cofactor for infection of monocytic cells, J. Immunol. 170 (9) (2003) 4840–4845.
[48] E. Farge, Increased vesicle endocytosis due to an increase in the plasma membrane phosphatidylserine concentration, Biophys. J. 69 (6) (1995) 2501.
[49] G.D. Fairn, M. Hermansson, P. Somerharju, S. Grinstein, Phosphatidylserine is polarized and required for proper Cdc42 localization and for development of cell polarity, Nat. Cell Biol. 13 (12) (2011) 1424–1430.
[50] S.-H. Lee, X.W. Meng, K.S. Flatten, D.A. Loegering, S.H. Kaufmann, Phosphatidylserine exposure during apoptosis reflects bidirectional trafficking between plasma membrane and cytoplasm, Cell Death Differ. 20 (1) (2013) 64–76.
[51] A. Dickey, R. Faller, Examining the contributions of lipid shape and headgroup charge on bilayer behavior, Biophys. J. 95 (6) (2008) 2636–2646.
[52] R.M. Venable, Y. Luo, K. Gawrisch, B. Roux, R.W. Pastor, Simulations of anionic lipid membranes: development of interaction-specific ion parameters and validation using nmr data, J. Phys. Chem. B 117 (35) (2013) 10183–10192.
[53] A. Velikonja, Š. Perutkova, E. Gongadze, P. Kramar, A. Polak, A. Maček-Lebar, A. Iglič, Monovalent ions and water dipoles in contact with dipolar zwitterionic lipid headgroups-theory and md simulations, Int. J. Mol. Sci. 14 (2) (2013) 2846–2861.
[54] E. Gongadze, U. van Rienen, A. Iglič, Generalized Stern models of an electric double layer considering the spatial variation of permittivity and finite size of ions in saturation regime, Cell. Mol. Biol. Lett. 16 (2011) (576–549).
[55] H. Fröhlich, Theory of Dielectrics, Clarendon Press, Oxford, UK, 1964.
[56] P. Budime Santhosh, A. Velikonja, c. Perutkova, E. Gongadze, M. Kulkarni, J. Genova, K. Eleršič, A. Iglič, V. Kralj-Iglič, N.P. Ulrih, Influence of nanoparticle-membrane electrostatic interactions on membrane fluidity and bending elasticity, Chem. Phys. Lipids 178 (2014) 52–62.
[57] E. Gongadze, U. Van Rienen, V. Kralj-Iglič, A. Iglič, Spatial variation of permittivity of an electrolyte solution in contact with a charged metal surface: a mini review, Comp. Methods Biomech. Biomed. Eng. 16 (5) (2013) 463–480.
[58] J. Deng, K.H. Schoenbach, E.S. Buescher, P.S. Hair, P.M. Fox, S.J. Beebe, The effects of intense submicrosecond electrical pulses on cells, Biophys. J. 84 (4) (2003) 2709–2714.
[59] L. Delemotte, M. Tarek, Molecular dynamics simulations of lipid membrane electroporation, J. Membr. Biol. 245 (9) (2012) 531–543.
[60] J.N. Sachs, P.S. Crozier, T.B. Woolf, Atomistic simulations of biologically realistic transmembrane potential gradients, J. Chem. Phys. 121 (22) (2004) 10847–10851.
[61] A.A. Gurtovenko, I. Vattulainen, Pore formation coupled to ion transport through lipid membranes as induced by transmembrane ionic charge imbalance: atomistic molecular dynamics study, J. Am. Chem. Soc. 127 (50) (2005) 17570–17571, http://dx.doi.org/10.1021/ja053129n (pMID: 16351063, URL http://dx.doi.org/10.1021/ja053129n).
[62] J. Pan, X. Cheng, L. Monticelli, F.A. Heberle, N. Kučerka, D.P. Tieleman, J. Katsaras, The molecular structure of a phosphatidylserine bilayer determined by scattering and molecular dynamics simulations, Soft Matter 10 (21) (2014) 3716–3725.
[63] P. Mukhopadhyay, L. Monticelli, D. Tieleman, Molecular dynamics simulation of a palmitoyl-oleoyl phosphatidylserine bilayer with Na^+ counterions and NaCl, Biophys. J. 86 (2004) 1601–1609, http://dx.doi.org/10.1016/S0006-3495(04)74227-7.
[64] J. Zelko, A. Iglič, V. Kralj-Iglič, S.P.B. Kumar, Effects of counterion size on the attraction between similarly charged surfaces, J. Chem. Phys. 133 (2010) 204901.